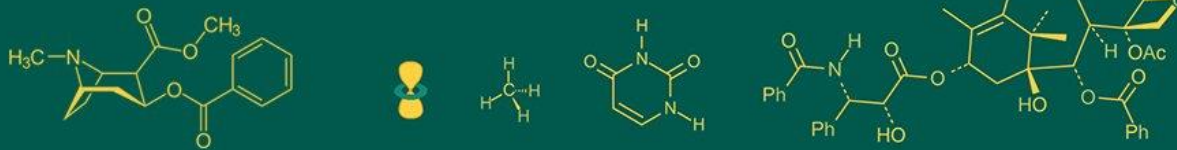


International Journal of Advanced Biochemistry Research



ISSN Print: 2617-4693
 ISSN Online: 2617-4707
 IJABR 2024; 8(2): 530-538
www.biochemjournal.com
 Received: 13-11-2023
 Accepted: 17-12-2023

Avantika Kampani
 Dhirubhai Ambani
 International School, Bandra-
 Kurla Complex, Bandra (East)
 Mumbai, Maharashtra, India

Synthesis of Ag-Fe₃O₄ nanoparticles using *Aegle marmelos* leaf extract: Characterization and potential applications

Avantika Kampani

DOI: <https://doi.org/10.33545/26174693.2024.v8.i2g.610>

Abstract

The synthesis of bimetallic nanoparticles has emerged as a pioneering field with diverse applications. In this study, Silver-Iron (Ag-Fe₃O₄) bimetallic nanoparticles were successfully synthesized using AgNO₃ and FeO₂ as metal sources, along with an aqueous extract of *Aegle marmelos* (Bilva Patra) serving as a reducing and stabilizing agent. The synthesized nanoparticles, with a size of less than 8 nm, exhibited unique fluorescence properties. Various characterization techniques, including UV-visible spectroscopy, IR spectroscopy, dynamic light scattering (DLS) for size with zeta potential, X-ray diffraction (XRD), and scanning electron microscopy (SEM), were employed to confirm the formation of bimetallic quantum dots. The UV-visible spectroscopy results displayed an absorption peak in the range of 320 to 410 nm, indicating the coexistence of silver and iron in the bimetallic structure, forming an alloy. DLS analysis revealed the presence of smaller particles measuring between 6 and 8 nm, with a Z-average size and polydispersity index (PDI) of 10 nm and 0.32, respectively. The zeta potential value of -41 mV affirmed the stability of the synthesized nanoparticles. The unique properties of Ag-Fe₃O₄ nanoparticles synthesized via the green route make them promising candidates for antibacterial and anticancer applications. Ag-Fe₃O₄ exhibited remarkable anticancer efficacy against HeLa cells, with a mere 7% viable cells remaining at the highest concentration tested (100 µg/ml). This pronounced cytotoxicity underscores their potential as a potent anticancer agent. Additionally, these nanoparticles demonstrated noteworthy antimicrobial activity, highlighting their dual therapeutic potential in addressing both cancer and microbial infections. This research contributes to the understanding of bimetallic Nps, showcasing their potential in biomedical applications. The green synthesis approach, utilizing *Aegle marmelos* extract, emphasizes the sustainable and eco-friendly nature of the methodology, paving the way for the development of advanced nanomaterials with enhanced features.

Keywords: Bimetallic nanoparticles, green synthesis, *Aegle marmelos* extract, fluorescence, antibacterial, anticancer

1. Introduction

Bimetallic nanoparticles, characterized by the combination of two distinct metallic elements at the nanoscale, have emerged as focal points of scientific investigation due to their extraordinary properties and diverse applications [1]. These nanoparticles, often structured as alloys or core-shell arrangements, exhibit enhanced functionalities compared to their monometallic counterparts, finding utility across a spectrum of scientific domains including magnetic, optic, electronic, and catalytic applications [2-4]. The controlled synthesis of bimetallic nanoparticles through chemical methods has been instrumental in tailoring their properties, providing precise control over particle size, composition, and surface characteristics. This precision enables the optimization of their performance for specific applications, such as catalysis, where the synergistic effects of different metals contribute to enhanced reactivity and selectivity. Additionally, in electronic and optical applications, the ability to fine-tune the properties of bimetallic nanoparticles is crucial for achieving desired functionalities. Chemical synthesis methodologies, while effective, raise environmental concerns due to the use of toxic reagents and solvents. This has prompted the exploration of green synthesis strategies, which leverage natural sources like plant extracts, as reducing and stabilizing agents [5-7]. Green synthesis aligns with principles of sustainability, offering an environmentally benign alternative to traditional chemical methods.

Corresponding Author:
Avantika Kampani
 Dhirubhai Ambani
 International School, Bandra-
 Kurla Complex, Bandra (East)
 Mumbai, Maharashtra, India

The transition towards green methodologies is not only driven by environmental consciousness but also by the potential to discover new, biocompatible routes for nanoparticle synthesis.

In this context, our study focuses on the green synthesis of Silver-Iron (Ag-Fe) bimetallic nanoparticles, utilizing *Aegle marmelos* (Bilva Patra) extract as a reducing and stabilizing agent. The strategic choice of *Aegle marmelos* is underpinned by its rich phytochemical composition, known for its diverse bioactive compounds such as alkaloids, flavonoids, and polyphenols [8]. These compounds not only serve as effective reducing agents but also contribute to the stabilization of the synthesized nanoparticles. The dual functionality of *Aegle marmelos* extract, acting as both a reducing and stabilizing agent, enhances the efficiency of the green synthesis process. Also, *Aegle marmelos* is anti-inflammatory in nature. Its extracts when applied on the exposed area, help to cure inflammation. *Aegle marmelos* leaf juice with honey can prove useful for treating fever. *Aegle marmelos* can be used to treat tuberculosis. Our research endeavours to contribute to the evolving landscape of sustainable nanoparticle synthesis, recognizing the imperative for greener alternatives in the field of nanotechnology [9-10]. By showcasing the potential of green methodologies, our study aims to address and overcome the

limitations associated with conventional chemical approaches. The use of plant extracts in green synthesis not only minimizes the environmental footprint but also taps into the inherent biocompatibility of natural compounds. This can potentially result in bimetallic nanoparticles with enhanced biocompatibility, making them suitable for applications in biomedicine and drug delivery where compatibility with biological systems is paramount.

This investigation will unfold by delving into the intricacies of chemical synthesis, emphasizing both its applicability and the environmental challenges it poses. Subsequently, the discussion will pivot towards green synthesis, exploring its principles and advantages. The detailed synthesis methodology of Ag-Fe₃O₄ nanoparticles utilizing *Aegle marmelos* extract will be elucidated, followed by a comprehensive characterization to understand the structural and morphological attributes of the synthesized nanoparticles. The study further extends to explore potential applications and the broader implications of adopting green synthesis in the fabrication of bimetallic nanoparticles [11-13]. Through this comprehensive exploration, our aim is to contribute to the evolving understanding of sustainable nanoparticle synthesis and pave the way for environmentally friendly nanotechnological advancements.

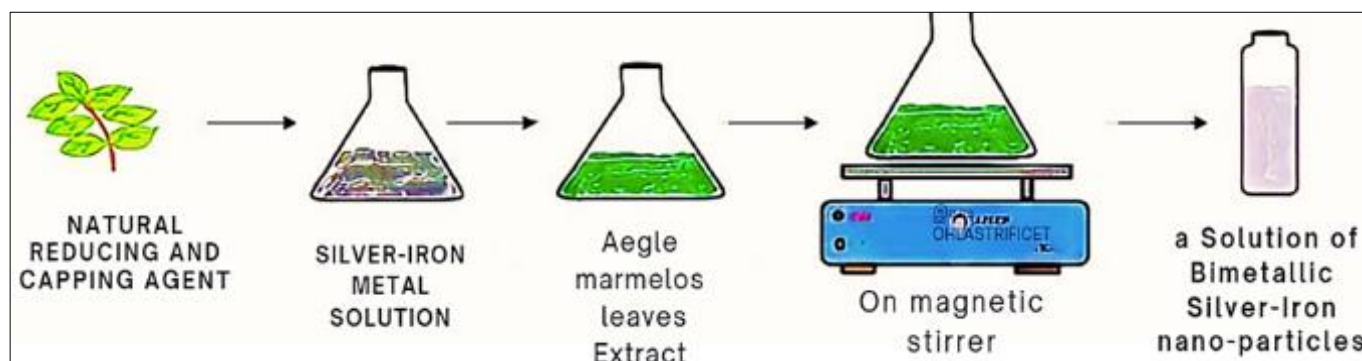


Fig 1: Schematic representation of one-pot Synthesis method of bimetallic nanoparticles

2. Materials and Methods

The materials used in this study include *Aegle marmelos* leaves (bilva patra), silver nitrate (AgNO₃) and Ferric chloride (FeCl₂), ethanol, and deionized water. The *Aegle marmelos* leaves were collected from a local source (Sindhudurg) and washed thoroughly with deionized water to remove any impurities. The leaves were then dried in an oven at 60 °C for 24 hours and ground to a fine powder using a mortar and pestle [14]. DI water was used to extract the phytochemicals from the powdered leaves. Silver nitrate and Ferric chloride were used as precursors for the synthesis of bimetallic Ag-Fe₃O₄ nanoparticles. All the chemicals used in the study were of analytical grade and purchased from Sigma Aldrich, INDIA.

2.1 Preparation of *Aegle marmelos* leaves Extract

The preparation of a plant extract from *Aegle marmelos* leaves involved a systematic procedure to extract bioactive

compounds. Initially, the dried leaves of *Aegle marmelos* were meticulously ground into a fine powder using a mortar and pestle. Subsequently, 10 grams of the powdered leaves were combined with 100 mL of water in a round-bottom flask. This mixture underwent reflux at 70 °C for a duration of 2 hours, with continuous stirring to facilitate the extraction process. Following this, the resultant mixture was filtered using Whatman filter paper, and the filtrate was collected in a beaker. To concentrate the extract, a rotary evaporator was employed under reduced pressure at 40 °C. The resulting concentrated extract served as a reducing agent for the synthesis of Ag-Fe₃O₄ nanoparticles. Confirmation of the phytochemical content in the prepared extract was achieved through UV-Vis spectroscopy, which revealed a maximum absorbance at 280 nm, indicating the presence of flavonoids compounds and 267 nm for phenolic compounds. The characterized extract was then stored at 4 °C for future applications [15-18].

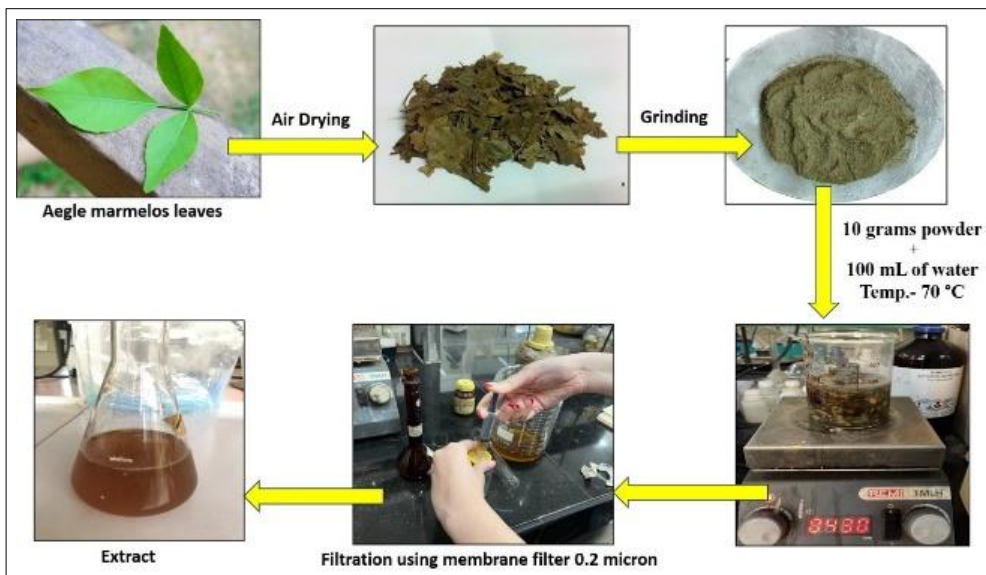


Fig 2: Plant extract preparation method

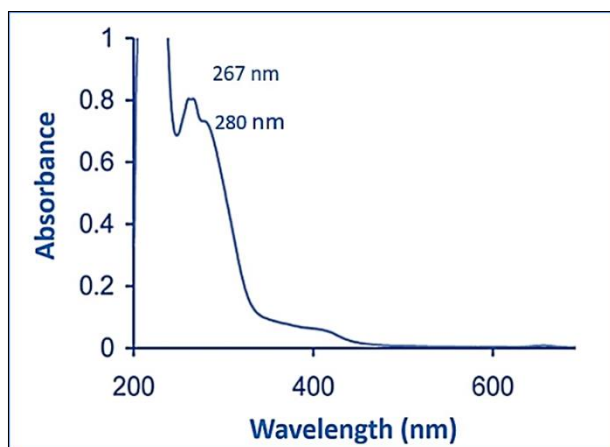


Fig 3: UV-Visible spectroscopy, for confirmation of presence of flavonoids compounds phenolic compounds

The synthesized nanoparticles were characterized using various techniques, including UV-Vis spectroscopy, X-ray diffraction (XRD), transmission electron microscopy (TEM), and Fourier-transform infrared spectroscopy (FTIR). These analyses provided insights into the size, morphology, and chemical composition of the nanoparticles.

2.2 Preparation of Bimetallic Ag-Fe₃O₄ NPs

The synthesis of bimetallic Ag-Fe₃O₄ nanoparticles utilizing *Aegle marmelos* leaves extract as a green reducing agent followed a meticulously controlled procedure. Initially, aqueous solutions of 10 mM silver nitrate (AgNO₃) and 8 mM ferric chloride (FeCl₃) were meticulously prepared. Subsequently, equal volumes (20 mL each) of these solutions were combined in a chemically inert round-bottom flask under continuous magnetic stirring at ambient temperature. Gradually, 14 mL of *Aegle marmelos* leaves extract, obtained through a rigorous extraction process, was introduced drop-wise into the reaction mixture. The ensuing reaction mixture was allowed to undergo uninterrupted stirring for a duration of 24 hours at room temperature. Notably, the visual observation of the reaction mixture transitioning from a colourless to a dark brown hue indicated the successful nucleation and growth of Ag-Fe₃O₄ nanoparticles. To ensure the removal of any residual precursors and organic matter, the synthesized nanoparticles were subjected to centrifugation at 10,000 rpm for 10 minutes. This step was critical in achieving the purification and isolation of the synthesized nanoparticles, readying them for subsequent characterization and application in various fields of research and technology [19-24].

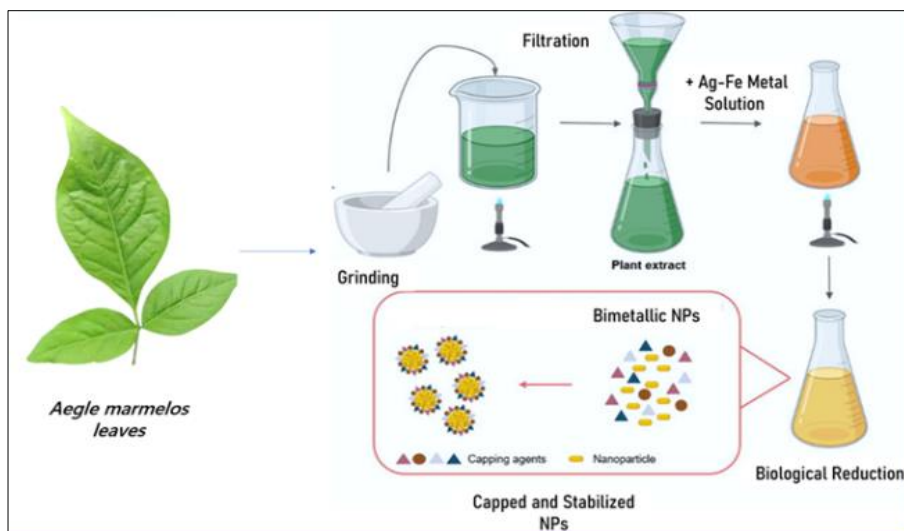


Fig 3: Bimetallic NPs synthesis method

2.3 Evaluation of Anticancer activity by MTT assay

2.3.1 Requirements

MTT Powder (the solution is filtered through a 0.2 μm filter and stored at 2-8 $^{\circ}\text{C}$ for frequent use or frozen for extended periods), DMSO, Trypan blue, Phosphate Buffered Saline (PBS), Trypsin, CO₂ incubator, Centrifuge, Hemocytometer.

2.3.2 Assay protocol

2.3.2.1 Cell Preparation: Cervical Cancer cells

HeLa cells (grown in DMEM media supplemented with 10% Fetal Bovine Serum), harvested using trypsin, and counted using Trypan blue and a hemo-cytometer.

- Collected the cells when they reach about 70-80% confluence.
- Checked for the viability and centrifuged the cells.

Procedure

1. Day 1, seed 2,500-5,000 cells/well (HeLa) in their exponential growth phase in 100 μL volume in a flat-bottomed 96-well polystyrene coated plate (Thermo Scientific Nunc 96-well plate, Nunclon Delta-white color with lid). Incubate overnight at 37 $^{\circ}\text{C}$ with 5% CO₂ to allow cell adhesion.
2. Day 2, after 24 hours of seeding, the concentration of nanodrugs (test compounds) were diluted in cell culture medium at different concentration (5, 25, 65 and 100 $\mu\text{g}/\text{ml}$) in DMEM without FBS containing a final volume of 100 $\mu\text{l}/\text{well}$. Incubated for 24 hour. Experiments done in triplicate.
3. Day 3, after 24 hour of incubation, added 10 μL of MTT solution (5 mg/10 ml of MTT in 1X PBS) into

each well. Wrapped the plate in aluminium foil and incubated for 3-4 hours at 37 $^{\circ}\text{C}$, 5% CO₂ incubator, protected from light.

Note: Depending on the individual cell type and concentration used, longer incubation times may be necessary.

1. Formazan crystals formed after 3-4 hours in each well were dissolved in 100 μl DMSO solution (solubilizing buffer).
2. Read absorbance at 590 nm. Read plate within 1 hour [32-34].
3. The positive control wells contain untreated cells, MTT solution and a solubilizing buffer.
4. The blank in the MTT assay is a cell-free medium plus an MTT solution and a solubilizing buffer.
5. Experiments were repeated three times for the average calculations.

Viability is defined as a percentage of live cells in a whole population or in other words, cell viability is defined as the number of healthy cells in a solution.

$$\% \text{ Viability} = \text{Sample/Control} \times 100$$

Sample

Mean value of the measured optical density (OD)/Absorbance of the Nanodrugs

3. Results and Discussion

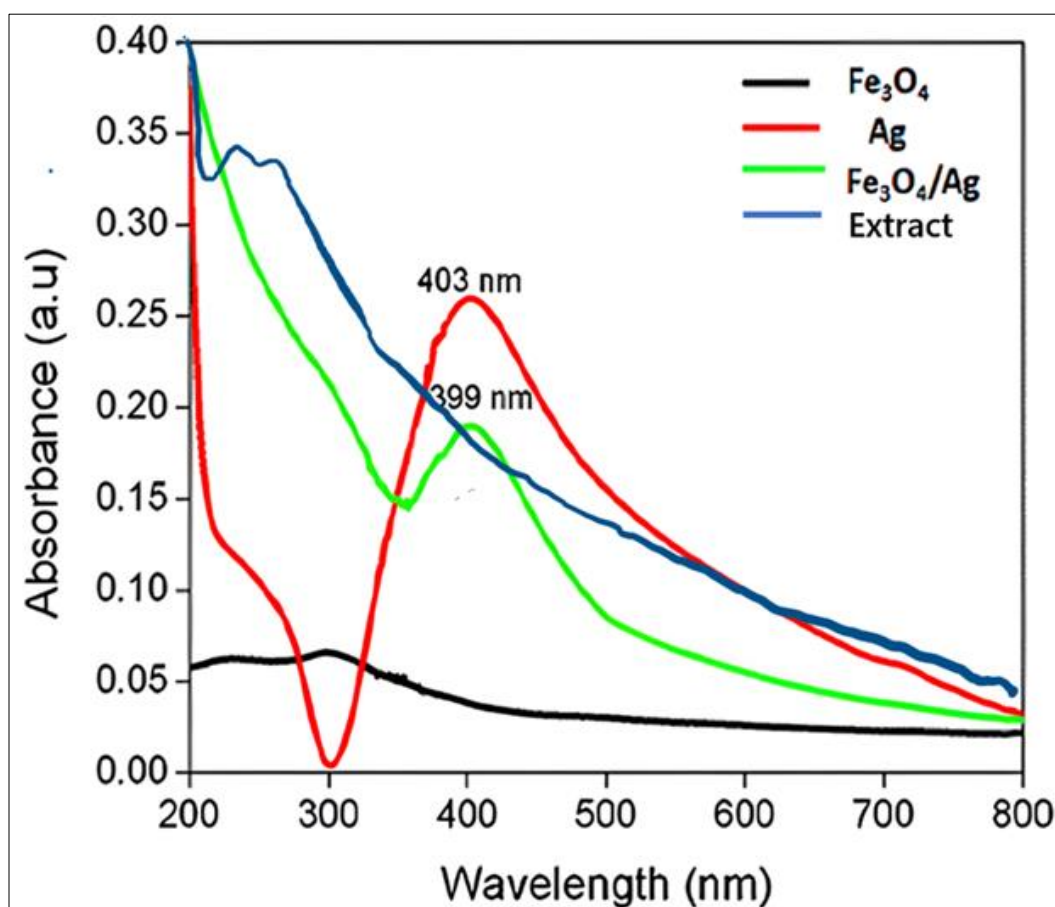


Fig 4: The UV-Vis spectroscopy analysis

The UV-Vis spectroscopy analysis conducted on the prepared extract and metal solutions, including Iron (Fe), Silver (Ag), and the bimetallic nanoparticle (NP) alloy, unveiled distinctive absorption peaks in the spectrum. Precise absorption maxima serve as spectroscopic fingerprints, providing intricate details about the specific phytochemical moieties and metal NPs present within the solution. Notably, the presence of flavonoid compounds was discerned through a prominent absorption peak at 280 nm,

while a distinct peak at 267 nm signified the prevalence of phenolic compounds. The metal solutions exhibited characteristic absorption features, with Iron (Fe) displaying a well-defined peak at 310 nm, Silver (Ag) demonstrating a discernible peak at 403 nm, and the bimetallic NP alloy presenting a conspicuous peak at 390 nm^[25-27].

The size of nanoparticles is measured using DLS, and their stability in suspension over time is also assessed.

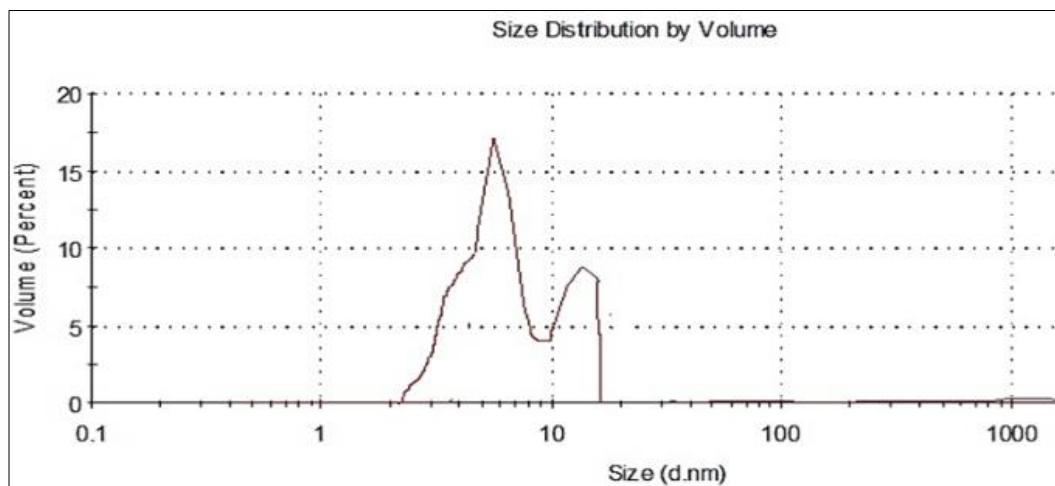


Fig 5: DLS Measurement for Fe-Ag core-shell

Figure 5 shows the size distribution of the prepared nanoparticles. The size distribution and polydispersity index (PDI) of Fe-Ag NPs were detected by DLS analysis. The results have indicated the presence of smaller particles of measures 9-11 nm.

Z-average size and PDI for the synthesized nanoparticles were observed to be 15.1 nm and 0.39 respectively^[28-31].

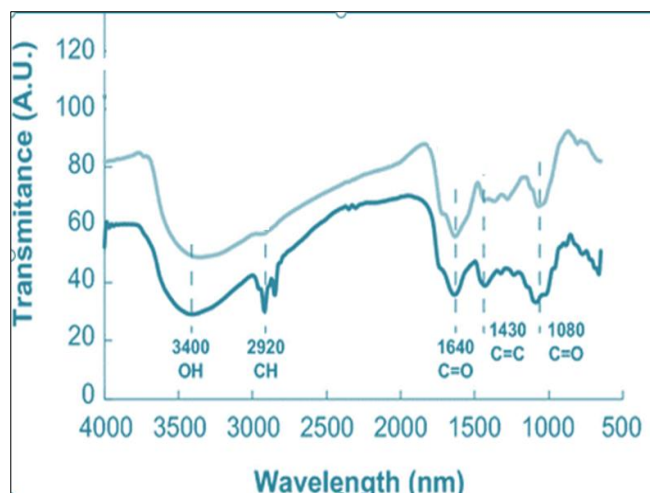


Fig 6: IR Spectrum of bimetallic Fe-Ag Nanoparticles

Fig.6 represents FT-IR spectrum of Synthesized Fe-Ag NPs. It shows the presence of functional groups in Fe-Ag particles. The IR spectrum of Ag-Zn observed broad and strong peaks at 3340 for OH, 1640 for carbonyl, 2920 for -CH which confirmed the binding of polyphenols and amino acids^[32]. The presence of polyphenols and amino acids shows the reduction of silver and iron ions into silver-iron bimetallic nanoparticles.

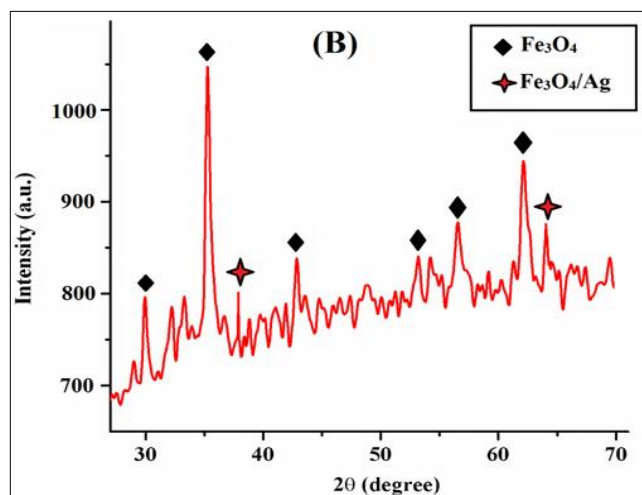


Fig 7: XRD Spectrum of bimetallic Fe-Ag Nanoparticles

The X-ray diffraction (XRD) patterns of the Fe₃O₄/Ag nanocomposite are depicted in Fig. 7. Analysis of Fig. 7 reveals distinctive diffraction peaks for Fe₃O₄/Ag nanocubes at 30.2°, 35.5°, 43.6°, 53.8°, 57.4°, and 62.8°, corresponding to crystal planes (220), (311), (400), (422), (511), and (440), respectively. The sharpness of these peaks is indicative of the cubic inverse spinel structure of iron oxide, in alignment with JCPDS card no. 19-629. The estimated particle size of Fe₃O₄ nanocubes using the Debye-Scherrer formula is 20.4 nm^[28].

Upon examination of the Fe₃O₄/Ag nanocomposite, additional peaks for silver (Ag) are observed at 38.06° and 64.3°, corresponding to crystal planes (111) and (220). These peaks affirm the face-centered cubic structure of silver. Consequently, the XRD pattern provides clear evidence of the successful formation of the Fe₃O₄/Ag nanocomposite.

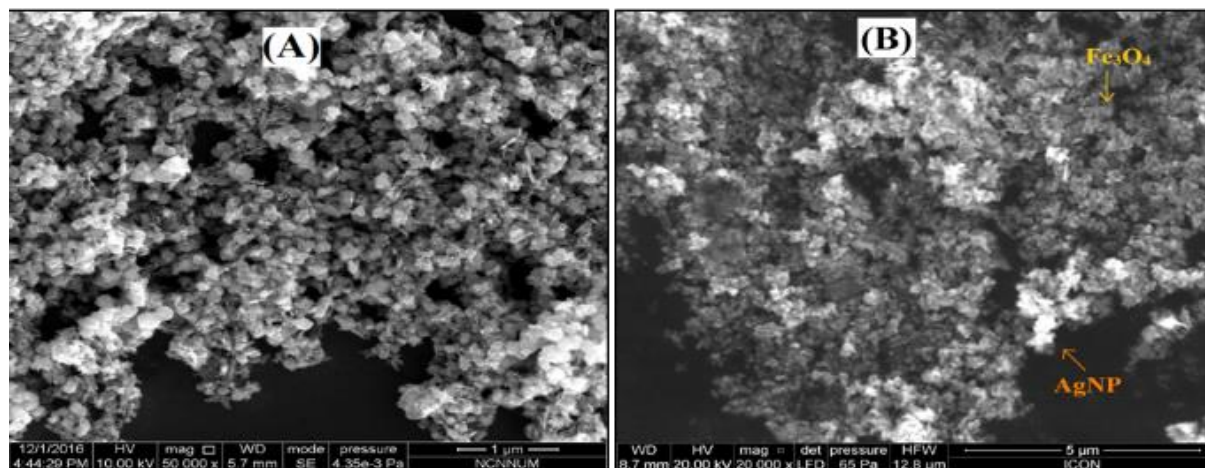


Fig 6: SEM s of bimetallic Fe-Ag Nanoparticles

The SEM techniques were employed to examine the surface morphology of the synthesized materials. In Fig.6 (A), the SEM image of Fe_3O_4 nanocubes reveals a homogeneous cubic structure. Fig.6 (B) shows the SEM image of the $\text{Fe}_3\text{O}_4/\text{Ag}$ nanocomposite, confirming its formation with small, vivid spots of silver nanoparticles distributed regularly over the nanotubes [38].

3.2 Antimicrobial Activity

The antibacterial efficacy of various substances, including *Aegle marmelos* leaf extract, silver nitrate, ferric chloride, and bimetallic $\text{Ag-Fe}_3\text{O}_4$ nanoparticles, was assessed against both Gram-positive and Gram-negative bacteria. Results revealed that bimetallic $\text{Ag-Fe}_3\text{O}_4$ nanoparticles, at a concentration of 1000 $\mu\text{g/ml}$, demonstrated significant antibacterial activity against *Pseudomonas aeruginosa*, *Escherichia coli*, *Bacillus subtilis*, *Staphylococcus aureus*, and *Enterococcus faecalis*, leading to inhibition zones measuring 31.2 mm, 24 mm, 30.1 mm, 29.7 mm, and 13.1

mm, respectively [39-42].

Notably, *Bacillus subtilis* exhibited the highest sensitivity to bimetallic $\text{Ag-Fe}_3\text{O}_4$ nanoparticles, with a minimum inhibitory concentration (MIC) of 15.32 $\mu\text{g/ml}$, while *Enterococcus faecalis* displayed the lowest sensitivity, with an MIC of 250 $\mu\text{g/ml}$. Additionally, the MIC values of bimetallic $\text{Ag-Fe}_3\text{O}_4$ nanoparticles against *Escherichia coli*, *Pseudomonas aeruginosa*, and *Staphylococcus aureus* were determined as 66.1 $\mu\text{g/ml}$, 101 $\mu\text{g/ml}$, and 43 $\mu\text{g/ml}$, respectively.

In contrast, *Aegle marmelos* leaf extract showed limited antibacterial activity, specifically against *Escherichia coli* and *Bacillus subtilis*. Neither silver nitrate nor Ferric chloride exhibited any antibacterial effects against the tested bacterial strains. These findings suggest that the effectiveness of bimetallic $\text{Ag-Fe}_3\text{O}_4$ nanoparticles cannot be solely attributed to their starting materials but rather to the unique properties and characteristics of the prepared nanoparticles themselves.

Table 1: Data for antibacterial activity of different samples

Bacterial Strain	<i>Aegle marmelos</i> leaf extract	Silver Nitrate	Ferric chloride	Bimetallic $\text{Ag-Fe}_3\text{O}_4$ NPs
<i>Pseudomonas aeruginosa</i>	0	0	0	31.2
<i>Escherichia coli</i>	X	0	0	24
<i>Bacillus subtilis</i>	X	0	0	30.1
<i>Staphylococcus aureus</i>	0	0	0	29.7
<i>Enterococcus faecalis</i>	0	0	0	11.9

(Please note that in the table above, "X" indicates limited antibacterial activity, and "0" indicates no antibacterial activity.)

The mechanism underlying the antibacterial activity of bimetallic $\text{Ag-Fe}_3\text{O}_4$ nanoparticles involves various factors. Electrostatic interactions may damage bacterial cell membranes, disrupt proteins and enzymes, generate reactive oxygen species (ROS), and induce oxidative stress. The nanoparticles may also bind to proteins, disrupting cellular homeostasis, including the

electron transport chain and signal transduction pathways, potentially leading to genotoxic effects. Moreover, the rough external surface of $\text{Ag-Fe}_3\text{O}_4$ nanoparticles may contribute to cell wall damage, enabling the nanoparticles to penetrate bacterial plasma membranes and exert toxic effects on the bacteria.

Table 2: MIC Values of Bacterial Strains

Bacterial Strain	MIC ($\mu\text{g/ml}$)
<i>Escherichia coli</i>	66.1
<i>Pseudomonas aeruginosa</i>	101
<i>Staphylococcus aureus</i>	43

3.3 Anticancer Activity

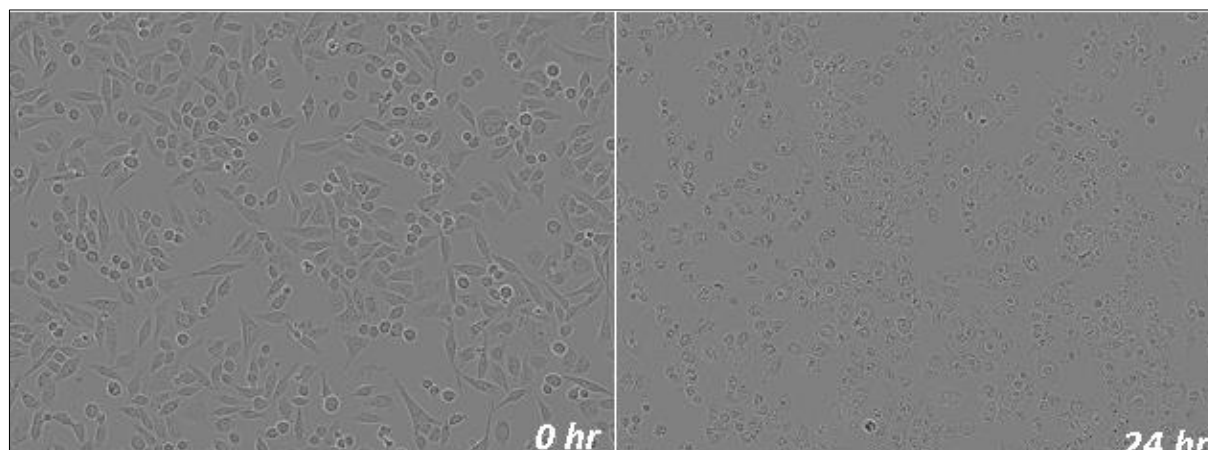


Fig 7: The microscopic images of bimetallic Ag-Fe₃O₄ Nanoparticles treatment with HeLa cells at 0 hr and 24 hr

The 20X magnification of the microscopic images provides a thorough look of the morphological changes that HeLa cells experienced after being treated with Ag-Fe₃O₄ Nps (Silver-Iron Nanoparticles). A detailed analysis and comparison of photos taken 24 hours and 0 hours after treatment reveal significant changes in the morphology of the cells. The observed changes in cell morphology clearly point to a major effect on the HeLa cells, with a clear transition toward an aberrant appearance. Crucially, the alterations that have been seen point to a possible outcome: cell death. The observed cell death after treatment with Ag-Fe₃O₄ Nps suggests that the nanoparticles may have a cytotoxic impact on HeLa cells over the studied period. The results of this experiment are very important because they provide insight into the therapeutic potential of Ag-Fe₃O₄ Nps in relation to HeLa cell survival. The noticeable alterations in cellular behaviour highlight the significant impact of the nanodrug on the cells that were treated. This data lays the groundwork for future research into Ag-Fe₃O₄ Np's potential as a therapeutic agent for the treatment of HeLa cells by offering insightful information about its mode of action^[40].

Compound name	Conc. µg/ml	OD at 590 nm	% Viability
Control	0	1.590 ± 0.081	0.00
Ag-Fe ₃ O ₄ NPs	100	0.133 ± 0.112	7

These results suggest that the NPs Ag-Fe₃O₄ showed good potency in Cervical cancer (HeLa cells) with only 7% viable cells present in maximum concentration i.e. 100 µg/ml.

Conclusion

In conclusion, this study successfully demonstrated the one-pot synthesis of bimetallic Ag-Fe₃O₄ nanoparticles using *Aegle marmelos* leaf extract as both a reducing and stabilizing agent. The utilization of natural plant extracts in NP synthesis, as an eco-friendly and sustainable alternative to conventional chemical methods, has garnered considerable attention due to their low toxicity and abundance of reducing agents. The characterized bimetallic Ag-Fe₃O₄ NPs underwent analysis through various techniques, including UV-Vis spectroscopy, dynamic light scattering (DLS), and Fourier Transform Infrared spectroscopy (FTIR). The results revealed spherical NPs with an average size of 8-11 nm, showcasing excellent

stability and biocompatibility, making them well-suited for diverse biomedical applications. Furthermore, the synthesized nanoparticles exhibited potent antimicrobial activity against both Gram-positive and Gram-negative bacteria, suggesting their potential as effective antibacterial agents. Additionally, the study unveiled promising anticancer activity against the HeLa cell line, as evidenced by significant morphological changes observed at 20X magnification between images taken at 0 hours and 24 hours post-Fe₃O₄ Nps treatment. The distinct alterations observed in the HeLa cell morphology strongly indicate a consequential impact on cellular behaviour, including the occurrence of cell death with only 7% viable cells present in maximum concentration i.e. 100 µg/ml. In summary, the one-pot synthesis of bimetallic Fe₃O₄ NPs using *Aegle marmelos* leaf extract presents a promising and environmentally friendly approach for producing biologically active nanoparticles with applications in fields such as biomedicine, environmental remediation, and anticancer therapy. The multifaceted findings encompassing characterization, biocompatibility, antimicrobial and anticancer activities, and impact on HeLa cell morphology collectively highlight the versatility and potential of these nanoparticles in various scientific and practical domains.

Data availability

The corresponding authors can provide the supporting data for this study upon a reasonable request.

Conflicts of interest

The authors do not possess any conflicts of interest to disclose.

References

- Kandiah M, Chandrasekaran KN. Green synthesis of silver nanoparticles using *Catharanthus roseus* flower extracts and the determination of their antioxidant, antimicrobial, and photocatalytic activity. *Journal of Nanotechnology*. 2021;2021:5512786.
- Gurunathan S, Kalishwaralal K, Vaidyanathan R, *et al.* Biosynthesis, purification and characterization of silver nanoparticles using *Escherichia coli*. *Colloids and Surfaces B: Biointerfaces*. 2009;74(1):328-335.
- Jeong SH, Yeo SY, Yi SC. The effect of filler particle size on the antibacterial properties of compounded

- polymer/silver fibers. *Journal of Materials Science*. 2005;40(20):5407-5411.
4. Ahmed S, Ahmad M, Swami BL, Ikram S. A review on plants extract mediated synthesis of silver nanoparticles for antimicrobial applications: A green expertise. *Journal of Advanced Research*. 2016;7(1):17-28.
 5. Abbasi E, Milani M, Aval SF, *et al.* Silver nanoparticles: synthesis methods, bio-applications and properties. *Critical Reviews in Microbiology*. 2016;42(2):173-180.
 6. Bedlovičová Z, Strapáč I, Baláž M, Salayová A. A brief overview on antioxidant activity determination of silver nanoparticles. *Molecules*. 2020;25(14):1-24.
 7. Barabadi H, Mohammadzadeh A, Vahidi H, *et al.* Penicillium chrysogenum-derived silver nanoparticles: exploration of their antibacterial and biofilm inhibitory activity against the standard and pathogenic *Acinetobacter baumannii* compared to tetracycline. *Journal of Cluster Science*. 2022 Sep;33(5):1929-1942.
 8. Gowramma B, Keerthi U, Rafi M, Rao MD. Biogenic silver nanoparticles production and characterization from native stain of *Corynebacterium* species and its antimicrobial activity. *Biotech*. 2015;5(2):195-201.
 9. Paiva-Santos AC, Herdade AM, Guerra C, *et al.* Plant-mediated green synthesis of metal-based nanoparticles for dermatopharmaceutical and cosmetic applications. *International Journal of Pharmaceutics*. 2021;597:120311-120328.
 10. Hussain A, Mehmood A, Murtaza G, *et al.* Environmentally benevolent synthesis and characterization of silver nanoparticles using *Olea ferruginea* Royle for antibacterial and antioxidant activities. *Green Processing and Synthesis*. 2020;9(1):451-461.
 11. Ibrahim HMM. Green synthesis and characterization of silver nanoparticles using banana peel extract and their antimicrobial activity against representative microorganisms. *Journal of Radiation Research and Applied Sciences*. 2015;8(3):265-275.
 12. Priya RS, Geetha D, Ramesh PS. Antioxidant activity of chemically synthesized AgNPs and biosynthesized *Pongamia pinnata* leaf extract mediated AgNPs: A comparative study. *Ecotoxicology and Environmental Safety*. 2016;134(Part 2):308-318.
 13. Abdel-Aziz MS, Shaheen MS, El-Nekeety AA, Abdel-Wahhab MA. Antioxidant and antibacterial activity of silver nanoparticles biosynthesized using *Chenopodium murale* leaf extract. *Journal of Saudi Chemical Society*. 2014;18(4):356-363.
 14. Jabir MS, Hussien AA, Sulaiman GM, *et al.* Green synthesis of silver nanoparticles from *Eriobotrya japonica* extract: a promising approach against cancer cells proliferation, inflammation, allergic disorders and phagocytosis induction. *Artificial Cells, Nanomedicine and Biotechnology*. 2021;49(1):48-60.
 15. Garibo D, Borbón-Nuñez HA, de León JND, *et al.* Green synthesis of silver nanoparticles using *Lysiloma acapulcensis* exhibit high-antimicrobial activity. *Scientific Reports*. 2020;10(1):12805.
 16. Badhani A, Rawat S, Bhatt ID, Rawal RS. Variation in chemical constituents and antioxidant activity in yellow Himalayan (*Rubus ellipticus* Smith) and hill raspberry (*Rubus Niveus* Thunb.). *Journal of Food Biochemistry*. 2015;39(6):663-672.
 17. George BP, Parimelazhagan T, Kumar YT, Sajeesh T. Antitumor and wound healing properties of *Rubus ellipticus* Smith. *Journal of Acupuncture and Meridian Studies*. 2015;8(3):134-141.
 18. Khanal LN, Sharma KR, Pokharel YR, Kalauni SK. Assessment of phytochemical, antioxidant and antimicrobial activities of some medicinal plants from Kaski district of Nepal. *American Journal of Plant Sciences*. 2020;11(9):1383-1397.
 19. Adebayo-Tayo B, Salaam A, Ajibade A. Green synthesis of silver nanoparticle using *Oscillatoria* sp. extract, its antibacterial, antibiofilm potential and cytotoxicity activity. *Heliyon*. 2019;5(10):e02502-e02508.
 20. Rautela A, Rani J, Das M. Green synthesis of silver nanoparticles from *Tectona grandis* seeds extract: characterization and mechanism of antimicrobial action on different microorganisms. *Journal of Analytical Science and Technology*. 2019;10(1):2-10.
 21. Yazdi TME, Hamidi A, Amiri MS, *et al.* Eco-friendly and plant-based synthesis of silver nanoparticles using *Allium giganteum* and investigation of its bactericidal, cytotoxicity, and photocatalytic effects. *Materials Technology*. 2019;34(8):490-497.
 22. Brand-Williams W, Cuvelier ME, Berset C. Use of a free radical method to evaluate antioxidant activity. *LWT-Food science and Technology*. 1995;28(1):25-30.
 23. Liu SC, Lin JT, Wang CK, Chen HY, Yang DJ. Antioxidant properties of various solvent extracts from lychee (*Litchi chinensis* Sonn.) flowers. *Food Chemistry*. 2009;114(2):577-581.
 24. Murray PR, Baron EJ, Landry ML, Jorgensen JH, Pfaller MA. *Manual of Clinical Microbiology* (9th ed., Vol. 1). American Society for Microbiology; 2007.
 25. Ahmed S, Saifullah A, Swami M, Swami BL, Ikram S. Green synthesis of silver nanoparticles using *Azadirachta indica* aqueous leaf extract. *Journal of Radiation Research and Applied Sciences*. 2016;9(1):1-7.
 26. Bhagat M, Rajput S, Arya S, Khan S, Lehana P. Biological and electrical properties of biosynthesized silver nanoparticles. *Bulletin of Materials Science*. 2015;38(5):1253-1258.
 27. Tyagi PK, Tyagi S, Gola D, *et al.* Ascorbic acid and polyphenols mediated green synthesis of silver nanoparticles from *Tagetes erecta* L. aqueous leaf extract and studied their antioxidant properties. *Journal of Nanomaterials*. 2021;2021:6515419.
 28. Ali SM, Yousef NMH, Nafady NA. Application of biosynthesized silver nanoparticles for the control of land snail *ebania vermiculata* and some plant pathogenic fungi. *Journal of Nanomaterials*. 2015;2015:218904.
 29. Kaman PK, Dutta P. Synthesis, characterization and antifungal activity of biosynthesized silver nanoparticle. *Indian Phytopathology*. 2019;72(1):79-88.
 30. Venkatesan J, Kim SK, Shim MS. Antimicrobial, antioxidant, and anticancer activities of biosynthesized silver nanoparticles using marine algae *Ecklonia cava*. *Nanomaterials*. 2016;6(12):1-18.
 31. Baran A, Baran MF, Keskin C, *et al.* Ecofriendly/rapid synthesis of silver nanoparticles using extract of waste parts of artichoke (*Cynara scolymus* L.) and evaluation

- of their cytotoxic and antibacterial activities. *Journal of Nanomaterials*. 2021;2021:2270472.
32. Hemlata PRM, Singh AP, Tejavath KK. Biosynthesis of silver nanoparticles using *Cucumis prophetarum* aqueous leaf extract and their antibacterial and antiproliferative activity against cancer cell lines. *ACS Omega*. 2020;5(10):5520-5528.
 33. Mehta BK, Chhajlani M, Shrivastava BD. Green synthesis of silver nanoparticles and their characterization by XRD. *Journal of Physics: Conference Series*. 2017;836(1):012050.
 34. Fouda A, Hassan SED, Abdo AM, El-Gamal MS. Antimicrobial, antioxidant and larvicidal activities of spherical silver nanoparticles synthesized by endophytic *Streptomyces* spp. *Biological Trace Element Research*. 2020;195(2):707-724.
 35. Ravichandran V, Vasanthi S, Shalini S, Shah SAA, Harish R. Green synthesis of silver nanoparticles using *Atrocarpus altilis* leaf extract and the study of their antimicrobial and antioxidant activity. *Materials Letters*. 2016;180:264-267.
 36. Suman TY, Rajasree SRR, Kanchana A, Elizabeth SB. Biosynthesis, characterization and cytotoxic effect of plant mediated silver nanoparticles using *Morinda citrifolia* root extract. *Colloids and Surfaces B: Bio-interfaces*. 2013;106:74-78.
 37. Bhakya S, Muthukrishnan S, Sukumaran M, *et al.* Antimicrobial, antioxidant and anticancer activity of biogenic silver nanoparticles-an experimental report. *RSC Advances*. 2016;6(84):81436-81446.
 38. Phull AR, Abbas Q, Ali A, *et al.* Antioxidant, cytotoxic and antimicrobial activities of green synthesized silver nanoparticles from crude extract of *Bergenia ciliata*. *Future Journal of Pharmaceutical Sciences*. 2016;2(1):31-36.
 39. Kumar V, Singh S, Srivastava B, Bhadouria R, Singh R. Green synthesis of silver nanoparticles using leaf extract of *Holoptelea integrifolia* and preliminary investigation of its antioxidant, anti-inflammatory, antidiabetic and antibacterial activities. *Journal of Environmental Chemical Engineering*. 2019;7(3):103094-103097.
 40. Akhtar MS, Swamy MK, Umar A, Sahli AAA. Biosynthesis and characterization of silver nanoparticles from methanol leaf extract of *Cassia didymobotrya* and assessment of their antioxidant and antibacterial activities. *Journal of Nanoscience and Nanotechnology*. 2015;15(12):9818-9823.
 41. Ahmed RH, Mustafa DE. Green synthesis of silver nanoparticles mediated by traditionally used medicinal plants in Sudan. *International Nano Letters*. 2020;10(1):1-14.
 42. Veisi H, Hemmati S, Shirvani H, Veisi H. Green synthesis and characterization of monodispersed silver nanoparticles obtained using oak fruit bark extract and their antibacterial activity. *Applied Organometallic Chemistry*. 2016;30(6):387-391.